

MODIFYING THE ASYNCHRONOUS JACOBI METHOD FOR DATA CORRUPTION RESILIENCE.*

CHRISTOPHER J. VOGL[†], ZACH ATKINS[‡], ALYSON FOX[§], AGNIESZKA MIĘDLAR[¶], AND COLIN PONCE^{||}

Abstract. Moving scientific computation from high-performance computing (HPC) and cloud computing (CC) environments to devices on the edge, where data can be collected by streamlined computing devices that are physically near instruments of interest, has garnered tremendous interest in recent years. Such edge computing environments can operate on data in-situ instead of requiring the collection of data in HPC and/or CC facilities, offering enticing benefits that include avoiding costs of transmission over potentially unreliable or slow networks, increased data privacy, and real-time data analysis. Before such benefits can be realized at scale, new fault tolerance approaches must be developed to address the inherent unreliability of edge computing environments, because the traditional approaches used by HPC and CC are not generally applicable to edge computing. Those traditional approaches commonly utilize checkpoint-and-restart and/or redundant-computation strategies that are not feasible for edge computing environments where data storage is limited and synchronization is costly. Motivated by prior algorithm-based fault tolerance approaches, an asynchronous Jacobi (ASJ) variant is developed herein with resilience to data corruption by leveraging existing convergence theory. The ASJ variant rejects solution approximations from neighbor devices if the distance between two successive approximations violates an analytic bound. Numerical results show the ASJ variant restores convergence in the presence of certain types of natural and malicious data corruption.

1. Introduction. Recent years have seen a proliferation of *edge devices*, i.e., streamlined computing devices that provide an entry point to the individual instruments they are near. Modern infrastructure includes a wide range of such devices, from smart residential thermostats to industrial smart grid meters. These devices, along with wearable healthcare devices and content delivery systems, are motivating a push of computation beyond the walls of high-performance (HPC) and cloud computing (CC) facilities onto the edge devices themselves. Consider, as an example, the benefits of enabling smart power grid devices to operate autonomously when the central operator is disabled due to a natural disaster or cyber-physical attack. The capabilities provided by edge computing environments to operate without a single point of failure or on data in-situ is very appealing to many real-time system operators. Unfortunately, the benefits of edge computing cannot be realized before the inherent unreliability of edge devices is addressed. Modern scientific computing algorithms typically assume that data will not be corrupted as the algorithm is executed. HPC and CC platforms provide such data integrity by utilizing fault management techniques. Checkpointing and redundant computation are cornerstones of fault management techniques in HPC and CC, and are an integral part of n-modular redundancy [4], n-version programming [12], majority voting [4], and redundant cloud servers [12] techniques. The frequency of checkpointing is typically chosen to avoid restarting from a checkpoint created long before the fault occurs while keeping the cost of synchronization and storage reasonable. Similarly, the amount of redundancy is typically chosen to avoid having all redundant entities experience a fault at the same time while keeping the cost of storage and flops reasonable. Thus, flop and storage limitations, along with heterogeneity of devices, can make checkpointing and redundancy approaches too expensive for practical use in edge computing environments.

One promising alternative fault management strategy is the class of *algorithm based fault tolerant*

*Submitted to the editors 15 June 2022.

Funding: This work was performed under the auspices of the U.S. Department of Energy by Lawrence Livermore National Laboratory under Contract DE-AC52-07NA27344 and was supported by the LLNL-LDRD Program under Project No. 21-FS-007 and 22-ERD-045, LLNL-JRNL-835736. The work of Agnieszka Międlar was supported by the NSF grant 181292.

[†]Lawrence Livermore National Laboratory, Livermore, CA (vogl2@llnl.gov)

[‡]Lawrence Livermore National Laboratory, Livermore, CA (atkins12@llnl.gov)

[§]Lawrence Livermore National Laboratory, Livermore, CA (fox33@llnl.gov)

[¶]University of Kansas, Lawrence, KS (amiedlar@ku.edu)

^{||}Lawrence Livermore National Laboratory, Livermore, CA (ponce11@llnl.gov)

(ABFT) methods. The general approach is to leverage the structure or expected behavior of the algorithm to detect, mitigate, and/or recover from faults such as data corruption. Examples of ABFT schemes include methods for the fast Fourier transform [11], matrix multiplication [16], Krylov-based iterative methods [6], and the synchronous Jacobi method [3]. Focusing on the iterative methods, the work presented in [6] uses the orthogonality of projections onto Krylov spaces for detection of faults, while [3] uses the contraction mapping property of stationary iterative methods. Unfortunately, those ABFT approaches are based on iterative methods that require frequent synchronizations, making them impractical for edge computing environments due to network latency, heterogeneous nodes, and nonpersistent nodes/links. Alternatively, ABFT approaches for asynchronous methods, such as linear systems solvers and optimization, remove the need for global synchronization after each iteration. The authors are aware of only two existing asynchronous methods with ABFT strategies: the robust alternating direction method of multipliers (ADMM) [10] and the robust push-sum algorithm [13].

To address the need for ABFT iterative methods for linear systems, we modify the Asynchronous Jacobi iteration [7, 8, 15, 3, 5] with a resilience modification technique that has been employed in [10], where ADMM convergence theory is used to reject corrupted data from neighboring nodes. Here, the theoretical analysis for the asynchronous Jacobi method in [8] is used to establish a rejection criterion based on the difference between successive data from a neighbor node. It is worthwhile to note that the Jacobi method is known to scale poorly to large and poorly-conditioned systems, and asynchronous Jacobi has the same limitations. However, Jacobi is often a core building block underlying more scalable solvers and is, in fact, often sufficient for many smaller problems that appear in edge environments. For these reasons, it is a logical target in developing asynchronous ABFT methods for linear systems.

This paper is organized as follows. Section 2 formulates the problem, introduces the notation and important definitions, and defines the data corruption to be investigated. Section 3 proposes our resilience enabling technique of interest. Section 4 presents numerical results verifying the implementation of the method and demonstrating the effectiveness of the rejection technique in the presence of various forms of data corruption. Section 5 summarizes the paper and discusses ongoing work.

2. Problem Statement. Solutions of linear systems are ubiquitous in modern scientific computing algorithms, defining search directions in both iterative and nonlinear solvers. Thus, consider solving the linear system

$$(2.1) \quad \mathbf{Ax} = \mathbf{b}$$

for $\mathbf{x} \in \mathbb{R}^m$, where $A \in \mathbb{R}^{m \times m}$ and $\mathbf{b} \in \mathbb{R}^m$. The asynchronous Jacobi method is an iterative solver for (2.1) in that successive approximations to \mathbf{x} are formed across N computational nodes. Denote by $\mathbf{x}_i \in \mathbb{R}^{m_i}$, where $m_i \leq m$, the block of \mathbf{x} that node i is approximating. Let $D \in \mathbb{R}^{m \times m}$ be the diagonal matrix containing the diagonal elements of A . The update equation that defines the successive approximations computed by node i , denoted $\mathbf{x}_i^0, \mathbf{x}_i^1$, etc., can now be expressed as

$$(2.2) \quad \mathbf{x}_i^\kappa = \sum_{j=1}^N M_{ij} \mathbf{x}_j^{\psi(i,j,\kappa)} + \mathbf{c}_i,$$

where $M_{ij} \in \mathbb{R}^{m_i \times m_j}$ is the (i, j) -th block of the iteration matrix $M := D^{-1}A$, $\mathbf{c}_i \in \mathbb{R}^{m_i}$ is the i -th block of $\mathbf{c} := D^{-1}\mathbf{b}$, and $\psi(i, j, \kappa) = m$ if node i uses node j 's m -th approximation in the computation of its κ -th approximation. The goal of this work is to modify (2.2) to ensure, or at least encourage, convergence even if data corruption results in the values of $\mathbf{x}_j^{\psi(i,j,\kappa)}$ received by node j are different than those sent by node i . As a convenience to the reader, Table 1 summarizes the notation used herein, as well as the location where the notation is first mentioned.

2.1. Natural Data Corruption. The first data corruption model is motivated by bit flips occurring in network hardware memory that corrupt data as it is in transit. This natural data corruption is

Table 1: Notation Table

Symbol	Description	Location
N	number of computational nodes	Section 2
A	square system matrix with real components, $\mathbb{R}^{m \times m}$	Section 2
D	diagonal matrix whose elements are the diagonal entries of A , $\mathbb{R}^{m \times m}$	Section 2
M	Jacobi iteration matrix $D^{-1}A$, $\mathbb{R}^{m \times m}$	Section 2
$M_{i,j}$	ij -th block of M	Section 2
i,j,k	blocks/elements	Section 2
λ, κ	iteration number, a nonnegative integer	Section 2
\mathbf{x}, \mathbf{b}	vectors of real components \mathbb{R}^m	Section 2
\mathbf{x}_i	vector containing the i -th block of elements of vector \mathbf{x} (assume that the i -th node is in charge of the i -th block of \mathbf{x})	Section 2
$\mathbf{x}_{i,k}$	the k -th element of the vector \mathbf{x}_i containing the i -th block of elements of vector \mathbf{x}	Section 2
\mathbf{x}_i^κ	the κ -th iteration of the i -th block of elements of vector \mathbf{x}	Section 2
$\psi_{ij}(\kappa) := \psi(i, j, \kappa)$	index of the update from node j which node i uses to compute its κ -th update	Section 2
p	the probability of a bit flip in a broadcasted element	Section 2.1
δ	an offset that is sampled from a Gaussian distribution with a positive mean	Section 2.2
ω_f, ω_r	the duration till a "down" or "normal" state for an agent	Section 2.2
$\nu_i(t)$	the iteration index such that $\mathbf{x}_i^{\nu_i(t)}$ is the most recent approximation on node i at time t	Section 3
$d\mathbf{x}_i^{\nu_i(t)} := \mathbf{x}_i^{\nu_i(t)} - \mathbf{x}_i^{\nu_i(t)-1}$	difference between two successive updates from the i -th block of elements	Section 3
ϵ	a user defined tolerance for the stopping criteria	Section 3
$\tilde{\mathbf{x}}(t)$	global approximate solution at time t such that $\tilde{\mathbf{x}}_i(t) = \mathbf{x}_i^{\nu_i(t)}$, $i = 1, \dots, N$	Section 3
\mathbf{x}^*	global exact solution to $A\mathbf{x} = \mathbf{b}$	Section 3
$\mathbf{e}(t)$	global error at time t such that $\mathbf{e}_i(t) = \tilde{\mathbf{x}}_i(t) - \mathbf{x}_i^*$	Section 3
$\kappa(A)$	condition number of matrix A	Section 3
$\Omega(t) := \Omega(\psi, M, t)$	error operator st $\mathbf{e}(t) = \Omega(t)\mathbf{e}(0)$	Section 3
$\mathcal{G}(\mathcal{V}, \mathcal{E})$	directed acyclic graph with nodes \mathcal{V} and edges \mathcal{E}	Section 3
$\tilde{s}_i(t)$	approximate shortest path	Section 3
$s(t), l(t)$	shortest and longest paths in \mathcal{G} , respectively	Section 3
$\tau_{ij}^{[k]}$	time at which the solution approximation existed on node j that will later be used to form \mathbf{x}_i^κ	Section 3
$\zeta_{ij}(t)$	$\arg \max_{\kappa} \psi_{ij}(\kappa) < \psi_{ij}(\nu_i(t))$	Section 3
$\sigma_{\min}(A), \sigma_{\max}(A)$	smallest and largest singular value of A	Section 3

modeled as a random process whereby each component of broadcasted data is affected by a bit flip with a fixed probability $p \in (0, 1)$. The bit flips themselves are performed either on IEEE 754 double precision (64 bit) floating point values [9] or on 32 bit signed integer values. The affected bit in each value is sampled from a uniform integer distribution, then the bit flip is performed directly. In exceedingly rare cases, this method of performing bit flips on double precision values can result in the special floating point values NaN or inf.

It is worth noting that this data corruption approach mirrors the model of Antz et al. [3]. Antz et al. introduce a fixed number of bit flips per iteration to the entries of the iteration matrix M during the matrix-vector product in each iteration, which may corrupt up to 1% of updates to the elements of the solution vector. We choose to instead corrupt the elements of the solution vector directly at a fixed probability $p \in (0, 1)$, i.e., corruption is applied with probability p to each broadcast data element.

2.2. Malevolent Data Corruption. The second data corruption model is motivated by intentional corruption caused by a malicious actor who has gained intermittent access to a device to manipulate the result of a calculation. This malevolent data corruption is modeled as a periodic process where each agent is considered to be in either a "normal" or a "down" state. When in a "normal" state, the new approximate solution is unaltered. After ω_f seconds have passed, the agent is compromised and enters a "down" state. While in the "down" state, the impacted data on an agent is corrupted by adding an offset to the solution elements. Note that such non-transient corruption, i.e., overwriting of the existing solution data, presents a more challenging recovery scenario than transient corruption. This offset is sampled from a Gaussian distribution with a positive mean δ and a standard deviation of 0.5δ . The repeated application of these offsets will gradually increase the magnitude of the corrupted elements of the solution vector, absent any mitigation strategy. We choose the standard deviation 0.5δ to ensure that 95% of the sampled offsets will be greater than zero regardless of the choice of δ . After ω_r seconds have passed, the agent is secured and returns to a "normal" state.

3. Modification Formulation. To improve data corruption resilience in the asynchronous Jacobi method (2.2), we take the approach of inspecting incoming data before it is used to form the next approximation to \mathbf{x}_i^κ in (2.2). If the data is identified as corrupted, it is rejected by being excluded from forming the next solution approximation. We will use the convergence theory established by Hook and Dingle [8] to derive our rejection criterion. Define $\nu_i(t)$ so that $\mathbf{x}_i^{\nu_i(t)}$ is the solution approximation on node i at time t . A global solution approximation at time t , denoted by $\tilde{\mathbf{x}}(t)$, is defined block-wise as $\tilde{\mathbf{x}}_i(t) = \mathbf{x}_i^{\nu_i(t)}$, $i = 1, \dots, N$. With \mathbf{x}^* being the exact solution of (2.1), the global error at time t is defined as $\mathbf{e}(t) = \tilde{\mathbf{x}}(t) - \mathbf{x}^*$. Denote the error operator $\Omega(\psi, M, t)$ such that $\mathbf{e}(t) = \Omega(\psi, M, t)\mathbf{e}(0)$. The properties of $\Omega(\psi, M, t)$, denoted herein as $\Omega(t)$, are presented in [8] using a directed acyclic graph $\mathcal{G}(\mathcal{V}, \mathcal{E})$ with graph nodes \mathcal{V} and edges \mathcal{E} . This is *not* the graph of computational node-to-node connections but is instead a directed acyclic graph representation of the evolution of the collective computation: each solution approximation at each computational node (i.e., each \mathbf{x}_j^κ) is an element of \mathcal{V} , and there is an edge in \mathcal{E} from \mathbf{x}_j^λ to \mathbf{x}_i^κ iff $\psi(i, j, \kappa) = \lambda$.

Given a non-negative iteration matrix M , i.e., all elements of M are non-negative, Hook and Dingle [8] show that $\Omega(t)$ is bounded as follows

$$(3.1) \quad \|\Omega(t)\|_2 \leq \left\| \sum_{k=s(t)}^{l(t)} M^k \right\|_2,$$

where $s(t)$ and $l(t)$ are the lengths of the shortest and longest paths in \mathcal{G} at time t , respectively. The goal now is to use (3.1) to develop a criterion for whether computational node i should accept or reject a new solution approximation $\mathbf{x}_j^{\psi(i, j, \nu_i(t))}$ obtained from node j . For notational brevity, we introduce $\psi_{ij}(\kappa) := \psi(i, j, \kappa)$.

To compare the new solution approximation $\mathbf{x}_j^{\psi_{ij}(\kappa)}$ to the previous solution approximation received by computational node i from computational node j , we define $\zeta_{ij}(t)$ to be the index of the solution approximation on node i that was last influenced by a solution approximation from node j . In other words, we seek to denote the two most recent solution approximations received by node i from node j at time t as $\mathbf{x}_j^{\psi_{ij}(\nu_i(t))}$ and $\mathbf{x}_j^{\psi_{ij}(\zeta_{ij}(t))}$, respectively. Formally, $\zeta_{ij}(t) = \arg \max_{\kappa} \{\psi_{ij}(\kappa) < \psi_{ij}(\nu_i(t))\}$. Now, a bound on $\|\mathbf{x}_j^{\psi_{ij}(\nu_i(t))} - \mathbf{x}_j^{\psi_{ij}(\zeta_{ij}(t))}\|_2$ can be derived using (3.1). Let $\tau_{ij}[\kappa]$ be the time at which the solution approximation existed on computational node j that would later be used to form \mathbf{x}_i^κ , and therefore $\nu_j(\tau_{ij}[\zeta_{ij}(t)]) = \psi_{ij}(\zeta_{ij}(t))$ and $\nu_j(\tau_{ij}[\nu_i(t)]) = \psi_{ij}(\nu_i(t))$. Note that $\mathbf{x}_j^{\psi_{ij}(\nu_i(t))}$ can now be expressed as $\mathbf{x}_j^{\nu_j(\tau_{ij}[\nu_i(t)])} = \mathbf{x}_j(\tau_{ij}[\nu_i(t)])$, and $\mathbf{x}_j^{\psi_{ij}(\zeta_{ij}(t))}$ can now be expressed as $\mathbf{x}_j^{\nu_j(\tau_{ij}[\zeta_{ij}(t)])} = \mathbf{x}_j(\tau_{ij}[\zeta_{ij}(t)])$. Thus, the following bound holds

$$\begin{aligned} \mathbf{x}_j^{\psi_{ij}(\nu_i(t))} - \mathbf{x}_j^{\psi_{ij}(\zeta_{ij}(t))} &= \underbrace{\mathbf{x}_j(\tau_{ij}[\nu_i(t)]) - \mathbf{x}_j^*}_{[\Omega(\tau_{ij}[\nu_i(t)])\mathbf{e}(0)]_j} + \underbrace{\mathbf{x}_j^* - \mathbf{x}_j(\tau_{ij}[\zeta_{ij}(t)])}_{[-\Omega(\tau_{ij}[\zeta_{ij}(t)])\mathbf{e}(0)]_j} \\ \Rightarrow \|\mathbf{x}_j^{\psi_{ij}(\nu_i(t))} - \mathbf{x}_j^{\psi_{ij}(\zeta_{ij}(t))}\|_2 &\leq \left[\|\Omega(\tau_{ij}[\zeta_{ij}(t)])\|_2 + \|\Omega(\tau_{ij}[\nu_i(t)])\|_2 \right] \|\mathbf{e}(0)\|_2 \end{aligned}$$

Assuming the initial solution approximation is the zero vector, one has $\|\mathbf{e}(0)\|_2 \leq \|A^{-1}\|_2 \|\mathbf{b}\|_2$. Assuming also that the iteration matrix M is non-negative, the Hook and Dingle bound (3.1) is now applied to obtain

$$(3.2) \quad \|\mathbf{x}_j^{\psi_{ij}(\nu_i(t))} - \mathbf{x}_j^{\psi_{ij}(\zeta_{ij}(t))}\|_2 \leq \left[\sum_{k=s(\tau_{ij}[\zeta_{ij}(t)])}^{l(\tau_{ij}[\zeta_{ij}(t)])} M^k + \sum_{k=s(\tau_{ij}[\nu_i(t)])}^{l(\tau_{ij}[\nu_i(t)])} M^k \right] \|A^{-1}\|_2 \|\mathbf{b}\|_2.$$

Evaluating the bound (3.2) directly is very difficult in practice, primarily because none of A^{-1} , the τ_{ij} map, nor the $s(t)$ and $l(t)$ functions are known *a priori*. Thus, to obtain a practical version of

(3.2), the two individual finite series are bounded by a single infinite series

$$\|\mathbf{x}_j^{\psi_{ij}(\nu_i(t))} - \mathbf{x}_j^{\psi_{ij}(\zeta(t))}\|_2 \leq 2\|A^{-1}\|_2\|\mathbf{b}\|_2 \sum_{k=s(\tau_{ij}[\zeta_{ij}(t)])}^{\infty} \|M\|_2^k.$$

Recall that $\|M\|_2$ is equal to the largest singular value of M , denoted $\sigma_{\max}(M)$, and that $\|A^{-1}\|_2$ is equal to the reciprocal of the smallest singular value of A , denoted $1/\sigma_{\min}(A)$. Finally, introduce $\tilde{s}_i(t)$ as a lower bound on $\min_{r \neq i} s(\tau_{ir}[\zeta_{ir}(t)])$, so that if the geometric series above converges (i.e., if $\|M\|_2 < 1$), it can be expressed as

$$(3.3) \quad \|\mathbf{x}_j^{\psi_{ij}(\nu_i(t))} - \mathbf{x}_j^{\psi_{ij}(\zeta(t))}\|_2 \leq 2 \frac{\|\mathbf{b}\|_2}{\sigma_{\min}(A)} \frac{\sigma_{\max}(M)^{\tilde{s}_i(t)}}{1 - \sigma_{\max}(M)},$$

where $\tilde{s}_i(t)$ is a lower bound on $\min_{r \neq i} s(\tau_{ir}[\zeta_{ir}(t)])$.

The lower bound $\tilde{s}_i(t)$ is obtained in the following manner: each computational node r sends its current value for $\tilde{s}_r(t)$ along with the current solution approximation to its neighbors. When computational node i receives a value for $\tilde{s}_r(t)$ from node r , that value is stored by node i as \tilde{s}_r . Additionally, every time node i computes a new solution approximation, a separate counter \tilde{s}_i^0 is incremented. Once computational node i has received a value from each neighbor r with $M_{ir} \neq 0$, the values for both $\tilde{s}_i(t)$ and \tilde{s}_i^0 are set to $\min(\tilde{s}_i^0, 1 + \min_{r: M_{ir} \neq 0} \tilde{s}_r)$. Then the process repeats, with computational node i again collecting updated values for all relevant $\tilde{s}_r(t)$ before updating $\tilde{s}_i(t)$. Note that since the value received from computational node j for $\tilde{s}_j(t) + 1$ should never be less than $\tilde{s}_i(t)$, the solution approximation $\mathbf{x}_j^{\psi_{ij}(\nu_i(t))}$ will only be accepted by computational node i if (3.3) is satisfied and the new value for $\tilde{s}_j(t)$ is such that $\tilde{s}_j(t) + 1 \geq \tilde{s}_i(t)$. This additional constraint provides some resilience for when the value of $\tilde{s}_j(t)$ is itself corrupted. These two constraints form the rejection criterion for the rejection variant of the asynchronous Jacobi method presented in Algorithm 1.

Algorithm 1: Asynchronous Jacobi Rejection Variant (ASJ-R)

```

1 foreach node  $i=1,2,\dots,N$  do
2   Initialize the algorithm with  $\mathbf{x}_i^0 = \mathbf{0}$ ,  $\tilde{s}_i = 0$ , and  $\tilde{s}_i^0 = 0$ . Set  $\kappa = 0$  and  $\mathcal{S} = \{\}$ .
3   foreach  $\mathbf{x}_j$  and  $\tilde{s}_j$  received from node  $j$  do
4     if  $\|\mathbf{x}_j - \mathbf{x}_j^\kappa\|_2 \leq 2 \frac{\|\mathbf{b}\|_2}{\sigma_{\min}(A)} \frac{\sigma_{\max}(M)^{\tilde{s}_i}}{1 - \sigma_{\max}(M)}$  and  $\tilde{s}_j + 1 \geq \tilde{s}_i$  then
5       set  $\mathbf{x}_j^\kappa = \mathbf{x}_j$ 
6       store  $\tilde{s}_j$  in  $\mathcal{S}$ 
7       if  $\mathcal{S}$  contains  $\tilde{s}_r$  for all  $r$  such that  $M_{ir} \neq 0$  then
8         set  $\tilde{s}_i = \min\{\tilde{s}_i^0, 1 + \min \mathcal{S}\}$ 
9         set  $\tilde{s}_i^0 = \tilde{s}_i$ 
10        set  $\mathcal{S} = \{\}$ 
11        set  $\mathbf{x}_i^{\kappa+1} = \sum_{r=1}^N M_{ir} \mathbf{x}_r^\kappa + \mathbf{c}_i$ 
12        set  $\tilde{s}_i^0 = \tilde{s}_i^0 + 1$ 
13        broadcast  $\mathbf{x}_i^{\kappa+1}$  and  $\tilde{s}_i$ 
14        set  $\kappa = \kappa + 1$ 

```

It is worth noting that developing appropriate stopping criteria for asynchronous methods remains an active area of research. Hook and Dingle [8] have each node report to a root node when a local stopping criterion is met. Each node will then continue iterating until hearing from the root node that all nodes have reported that the local criterion has been met. Our approach uses a similar local stopping criterion as Hook and Dingle but replaces the root node approach with a decentralized “convergence duration.” The iteration loop on a given node is executed until either a given maximum number of

iterations is reached or at least 1 second has passed since all other nodes have broadcasted that they have met the local stopping criterion

$$(3.4) \quad \|D_{ii}d\mathbf{x}_i^{\nu_i(t)}\|_\infty < \epsilon \frac{\|b\|_2}{\sqrt{m}},$$

where $d\mathbf{x}_i^{\nu_i(t)} = \mathbf{x}_i^{\nu_i(t)} - \mathbf{x}_i^{\nu_i(t)-1}$ and ϵ is a prescribed tolerance. Note that when used for parallel synchronous Jacobi, the local stopping criterion (3.4) does indeed imply that $\|\mathbf{e}(t)\|_2 \leq \epsilon\kappa(A)\|\mathbf{b}\|_2$, where $\kappa(A)$ is the condition number of matrix A (see [8]); however, this is not guaranteed for its asynchronous counterpart. Despite the lack of guarantee, we do empirically find for the problems herein that (i) (3.4) does result in relative global errors of order $\epsilon\kappa(A)$ and (ii) the 1 second ‘‘convergence duration’’ is long enough for all the nodes to ‘‘agree’’ on global convergence, i.e., all nodes have decided to stop at a time t where (3.4) is satisfied for all i ’s. It should be noted that the ‘‘convergence duration’’ is likely dependent on the computational hardware and linear system size, e.g., slower hardware and larger system sizes that result in longer intervals between solution approximations might require a longer ‘‘convergence duration.’’

4. Numerical Results. Having derived the modified asynchronous Jacobi in Section 3, shown in Algorithm 1, we now evaluate and validate the method on a benchmark problem. We chose the benchmark to have an analytic solution so we can verify the implementation of Algorithm 1. We then evaluate the method performance against that of the traditional asynchronous Jacobi method when the natural and malevolent data corruption described in Sections 2.1 and 2.2, respectively, are present. Each run is performed on a single 36-core node of the Quartz supercomputer at the Livermore Computing Complex.

The linear system (2.1) solved throughout this section is obtained from a finite difference discretization of the following Poisson problem on the unit square

$$(4.1) \quad \begin{aligned} -\left(\frac{\partial^2 u}{\partial x^2} + \frac{\partial^2 u}{\partial y^2}\right) &= f, \quad x \in (0, 1), y \in (0, 1), \\ u(0, y) = u(1, y) = u(x, 0) = u(x, 1) &= 0, \end{aligned}$$

where $f(x, y) = 2\pi^2 \sin(\pi x) \sin(\pi y)$ results in an analytic solution $u(x, y) = \sin(\pi x) \sin(\pi y)$. The unit square is uniformly discretized, resulting in $\ell + 1 \times \ell + 1$ squares of length $h = 1/(\ell + 1)$. Such a discretization along with the Dirichlet boundary condition in (4.1) leaves the values of $u(x_i, y_j)$, where $x_i = (i + 1)h$ and $y_j = (j + 1)h$ for $i = 0, \dots, \ell - 1$ and $j = 0, \dots, \ell - 1$, to be determined. Let the k -th element of $\mathbf{x} \in \mathbb{R}^{\ell^2}$ and $\mathbf{b} \in \mathbb{R}^{\ell^2}$ in (2.1) be $u(x_i, y_j)$ and $f(x_i, y_j)$, respectively, with $i = (k \bmod \ell)$ and $j = k\ell$. With the Laplace operator discretized across the nodes (x_i, y_j) using centered finite difference, the matrix A in (2.1) can be reformulated as the following $\ell^2 \times \ell^2$ block tridiagonal matrix

$$A = \begin{bmatrix} D & -I & & & \\ -I & D & -I & & \\ & \ddots & \ddots & \ddots & \\ & & -I & D & -I \\ & & & -I & D \end{bmatrix}, \text{ where } D = \begin{bmatrix} 4 & -1 & & & \\ -1 & 4 & -1 & & \\ & \ddots & \ddots & \ddots & \\ & & -1 & 4 & -1 \\ & & & -1 & 4 \end{bmatrix}$$

and I is the $\ell \times \ell$ identity matrix.

4.1. Implementation: Collaborative Autonomy and Skywing. The work presented in this paper is part of an emerging class of methods known as *collaborative autonomy*, which is aimed at enabling decentralized, unstructured groups of computers to self-organize in order to collectively solve computational problems in a manner that can adapt around unreliabilities in the computing environment. While there is preexisting software that accomplishes some of the tasks that are required

of collaborative autonomy, none accomplishes all of them. Perhaps the most similar is the class of open-source, distributed cluster-computing frameworks that include Apache Hadoop [1] and Apache Spark [2]. These frameworks are designed for large-scale, “big data” computing work, implement leader-follower patterns, perform computing in batches, and while they have some fault tolerance, they are not inherently resilient to common faults in edge computing applications, such as hardware faults and cyber intrusions. Another related class is HPC-focused platforms such as OpenMP and MPI that are commonly used to enable parallel computing; however, these frameworks also lack tolerance for common unreliability in edge computing environments and are not designed for streaming computing.

To support the needs of collaborative autonomy and resilient, streaming edge computing, Lawrence Livermore National Laboratory has developed the *Skywing* software platform. Instead of point-to-point messaging, Skywing communicates via a “publisher-agnostic” publication and subscription model over TCP/IP and provides functionality for facilitating the implementation of unstructured, asynchronous collective iterative methods, as well as a number of such iterative methods. A key feature in Skywing is its *method composition* module, which enables the construction of more-complex asynchronous iterative methods by using simpler asynchronous iterative methods as building blocks. When iterative methods are built using resilient collective methods as building blocks, the resulting iterative methods inherits the resilience of its underlying components. The methods in this paper were implemented in Skywing which is open source and available on GitHub [14].

4.2. Experimental Verification. The implementation of both the traditional asynchronous Jacobi (ASJ) and ASJ-R algorithms are first verified on the benchmark problem (4.1) by ensuring the numerical solutions match the analytic solution to within tolerance for a variety of system sizes: $\ell = \{4, 5, 6, 7, 8, 9, 10, 11, 12, 20, 25, 30\}$. These verification experiments use discrete Poisson matrices $A \in \mathbb{R}^{m \times m}$ with m ranging from 8 to 150 rows. Additionally, each system is tested with its rows evenly distributed among 4, 8, and 16 agents. Figure 1 shows the dependence of the wall-clock time for convergence on the condition number of A for each of the system sizes considered. Each data point is the average across 10 trials using the geometric mean. We define the geometric mean as

$$\bar{a} = \exp\left(\frac{1}{s} \sum_{k=1}^s \log(a_k)\right).$$

We see that after the system size reaches a sufficient size, the condition number dominates the growth of the number of iterations required for convergence. Specifically, a clear linear relationship between the wall-clock time and $\kappa(A)$ is observed. Moreover, the wall-clock time remains constant despite increasing the number of agents, which is the expected scaling behavior of the asynchronous Jacobi algorithm.

4.3. Path Length Rejection Variant with Data Corruption. We evaluate the resilience of the ASJ rejection variant (ASJ-R) to both bit flip and malevolent corruption, as defined in Section 2.1 and Section 2.2, respectively. All experiments solve (4.1) on a mesh with 20×20 interior discretization points ($\ell = 20$) distributed evenly over 16 Skywing agents. We choose to use a small number of agents relative to experiments targeting HPC systems, e.g., [3], due to our intended application area of collaborative autonomy with edge devices. Such devices will not be able to capitalize on the numerous processor cores and high-speed interconnects of HPC system and, thus, will primarily utilize small neighborhoods of communicating devices.

Natural Data Corruption. Our first scenario introduces transient bit flips to computed data, similar to the experiments performed by Antz et al. in [3]. We aim to assess the impact of the probability p of a bit flip on the performance and convergence of ASJ-R compared to traditional ASJ. As discussed in Section 2.1, corruption is applied at each iteration and on every agent with probability p to all broadcasted data. The elements of \mathbf{x}_i^k are stored as IEEE 754 double floating point numbers whereas the values of \tilde{s}_i are stored as signed integers. If a given data value is chosen to be corrupted, a random index out of its 64 bit or 32 bit representation is chosen to be flipped. For our first experiment, we allow

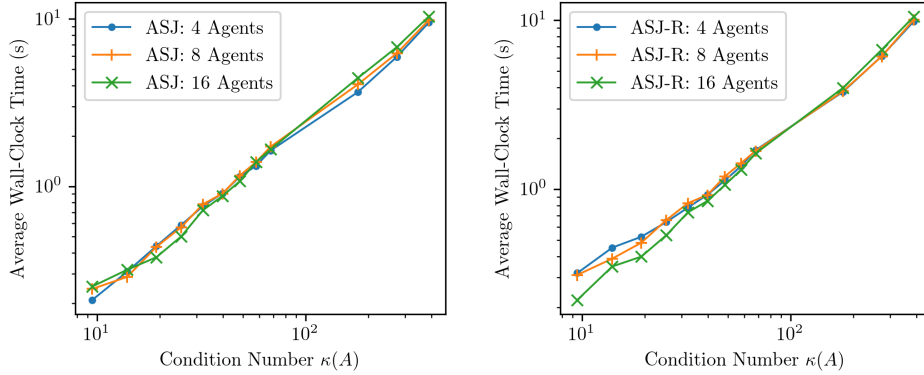


Fig. 1: Scaling of wall-clock time with respect to the condition number for $\ell = \{4, 5, 6, 7, 8, 9, 10, 11, 12, 20, 25, 30\}$. The average wall-clock time is reported using the geometric mean of 10 trials. The left plot depicts the results for ASJ while the right plots depicts the results for ASJ-R.

bit flips in any of the 64 bits of the double and any 32 bits of the integer. Figure 2 shows the performance of ASJ-R with a range of bit flip probabilities. Even when an extremely high number of bit flips occur, e.g. 4% of broadcasted data are corrupted at each iteration, the ASJ-R algorithm still converges and does so around twice the time of the algorithm absent corruption. The delay introduced by the ASJ-R algorithm only moderately affects the scaling with respect to the frequency of bit flips. Note that for all tested probabilities, the error remains stagnant for a fixed period before rapidly converging. This stagnation period represents the time needed for the shortest path length estimates \tilde{s}_i to increase to a value where the rejection criterion is strict enough for the corruption. Once there is sufficient rejection of data corruption, convergence behavior is restored.

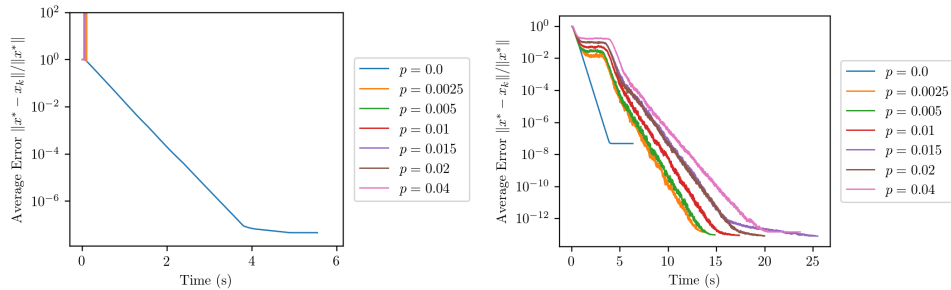


Fig. 2: Convergence for 16 agents with bit flip probabilities of $p \in \{0\%, 0.25\%, 0.5\%, 1\%, 1.5\%, 2\%, 4\%\}$. The average relative error is reported using the geometric mean of 10 trials. The left plot depicts the results for ASJ while the right plot depicts the results for ASJ-R.

We also consider the effects of bit flips occurring at different positions of the IEEE 754 double representation, as was done by Antz et al. in [3]. We distinguish between corruptions that flip any of the 64 bits $\text{IE}^3([0-63])$ and corruptions that flip only a specific subset of the bits, i.e., corruptions which occur only in the lower mantissa $\text{IE}^3([0-25])$, the upper mantissa $\text{IE}^3([26-51])$, the exponent $\text{IE}^3([52-62])$, or the sign bit $\text{IE}^3(63)$. Figure 3 shows the convergence of ASJ and ASJ-R under each type of bit flip, occurring with a probability of $p = 0.01$. The traditional variant only converges for bit flips occurring in the lower mantissa, consistent with the results in [3], which found that lower-mantissa

bit flips only affect convergence to a high tolerance. The traditional variant quickly diverges to NaN values in Figure 3c, reflected in the plot as the algorithm terminating almost immediately. Conversely, the ASJ-R algorithm converged for every type of bit flip, albeit with a marginally larger convergence delay for bit flips in the upper mantissa. In Figures 3b, 3c, and 3d, ASJ-R required approximately twice the amount of time to converge, with the first half of the time showing little progress. As before, the stagnation is a result of waiting for the shortest path length estimates to reach a level for corruption rejection.

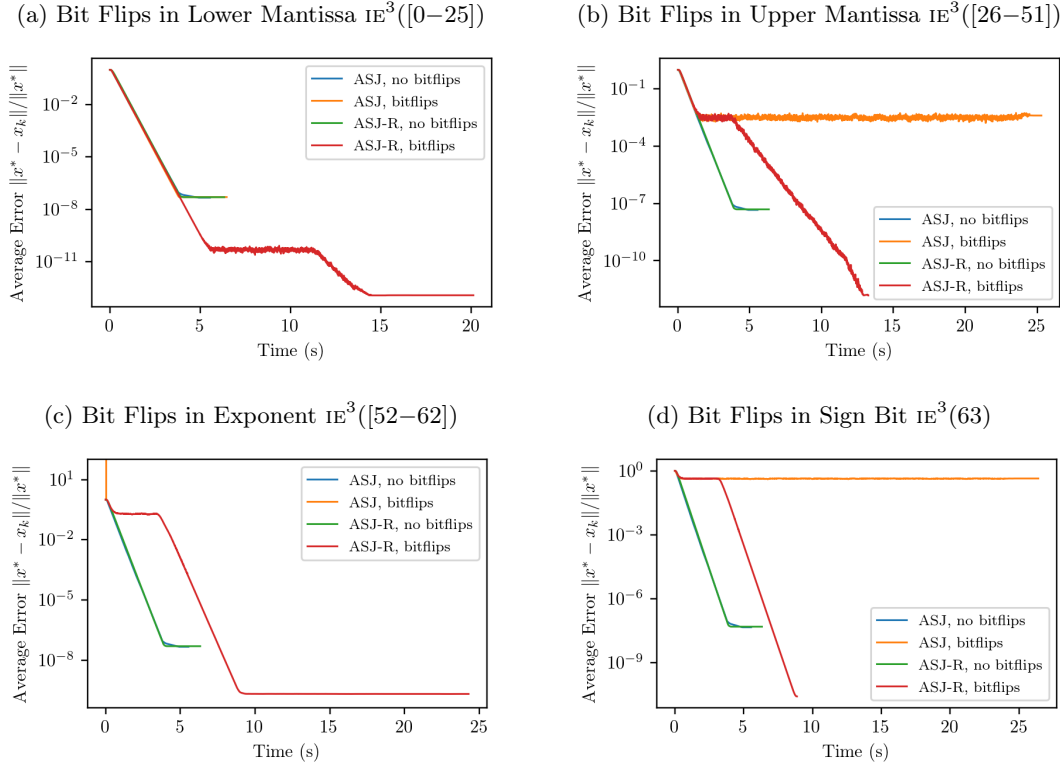


Fig. 3: Traditional ASJ vs. ASJ-R variant for different bit flip locations with fixed bit flip probability $p = 0.01$ on the 2D Poisson test problem distributed over 16 agents. The geometric mean of the relative error is reported for 15 runs per ensemble

Malevolent Data Corruption. Our second scenario models a malevolent actor who gains intermittent access to a device seeking to manipulate the result of a calculation, as described in Section 2.2. We aim to assess the impact of the recovery time ω_r and mean of the randomly sampled offset δ on the performance and convergence of ASJ-R compared to traditional ASJ. As described in Section 2.2, while an agent is in the degraded state, every element in \mathbf{x}_i^k has an offset added to it sampled from a normal distribution with mean δ and standard deviation 0.5δ . The time-to-failure ω_f of the data corruption is chosen by considering both the convergence duration in the stopping criterion (3.4) and the typical time the ASJ method takes to converge in the absence of data corruption. Note that a ω_f value less than the convergence duration will essentially mean no convergence, while a ω_f value greater than the time it takes to converge in the absence of data corruption will essentially guarantee convergence.

We first evaluate the effect of the offset mean δ on convergence. Figure 4 shows the convergence profiles of 10-run ensembles of both traditional ASJ and ASJ-R with a range of values of δ . For all

experiments, the malevolent corruption is applied with a time-to-failure $\omega_f = 2.5$ seconds and recovery time $\omega_r = 0.2$ seconds. Under these parameters, traditional ASJ fails to converge for any tested mean δ . Conversely, all runs of ASJ-R converge for all tested values of δ . In particular, the algorithm converges in less than twice the time required for convergence without any corruption, which is particularly promising. The rejection criteria allows for the relative error to return to the pre-corrupted magnitude almost immediately, mitigating further slowdowns.

The ASJ-R criterion is, however, potentially too strong for this kind of corruption in certain cases, e.g., for sufficiently small or large values of δ . In such cases, we noted the algorithm rejecting all solution approximations from a corrupted agent, even after the corrupted period ends. Such behavior effectively cut off the corrupted agent from the computation, leading to stagnated convergence. Avoiding this aggressive rejection might require a better approximation of the shortest path length $s(t)$ or introducing dynamic adjustment to the rejection criterion that weakens the criterion if solution approximations from one agent are consistently rejected. Additionally, Figure 5 shows the convergence profile of ASJ-R for a different values of the recovery time parameter ω_r . Each of the 10-run ensembles uses a time-to-failure of $\omega_f = 2.5$ seconds and a mean $\delta = 0.2$. Overall, the recovery time appears to have very little impact on the convergence behavior within the tested range. However, sufficiently large recovery time values lead to the same issues as with too aggressive rejection as described above.

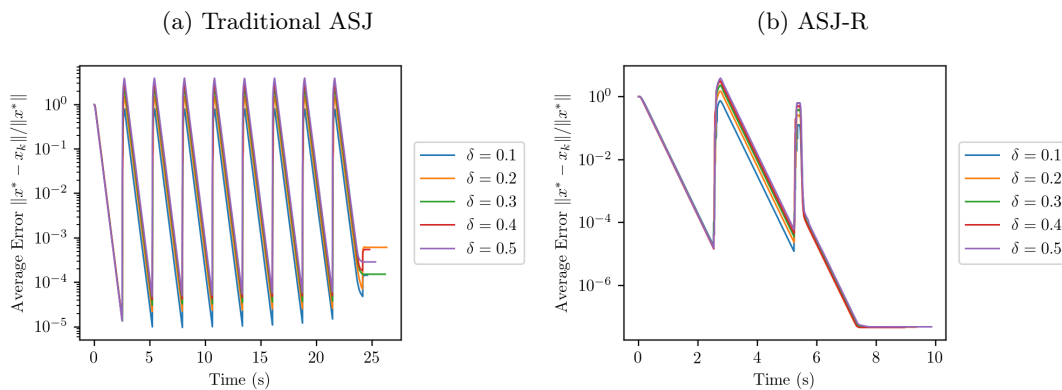


Fig. 4: Convergence results for traditional ASJ (left) and ASJ-R (right) on the 400×400 2D Poisson benchmark distributed over 16 agents, with malevolent data corruption on agent 8 with $\omega_f = 2.5$ seconds, $\omega_r = 0.2$ seconds, and $\delta \in \{0.1, 0.2, 0.3, 0.4, 0.5\}$. The geometric mean of the relative error is reported for 10 runs per ensemble.

5. Conclusions. In this paper, we have introduced a fault-tolerant Asynchronous Jacobi (ASJ) variant that leverages ASJ convergence theory by Hook and Dingle [8] to provide resilience to data corruption. The resulting ASJ Rejection Variant (ASJ-R) strategy rejects solution approximations from neighbor nodes if the distance between two successive approximations violates an analytic bound. We have implemented the fault-tolerant asynchronous algorithm using the recently developed Skywing software library at Lawrence Livermore National Laboratory for collaborative autonomy and performed a comprehensive numerical study to evaluate the proposed resilience strategy. We showed that in the presence of natural (bit flips) and malicious (intended data manipulation) data corruption, ASJ-R recovers the convergence behavior of the traditional ASJ method. We note that even when an extremely high number of bit flips occur, the ASJ-R algorithm still converges and does so around twice the time of the algorithm absent corruption. While this slowdown is larger than that observed by Antz et al. [3] in their algorithm, ASJ-R has the added benefit of detecting and mitigating other forms of corruption besides bit flips, such as malevolent data corruptions. We did note that ASJ-R did not converge when

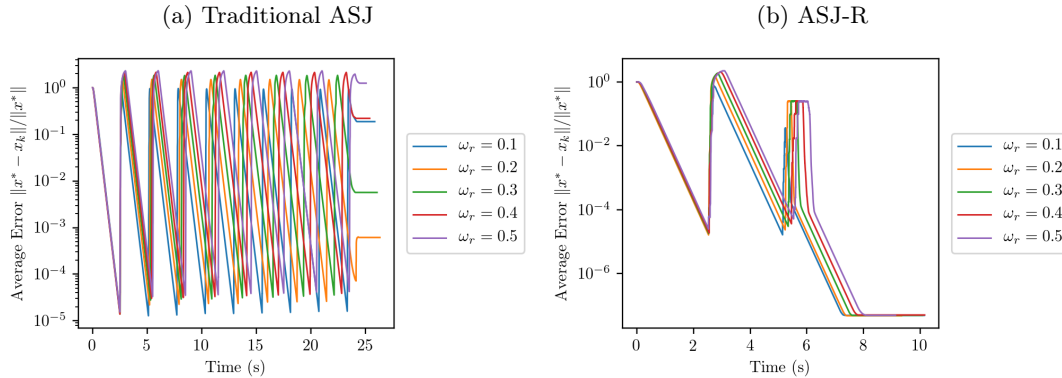


Fig. 5: Convergence results for traditional ASJ (left) and ASJ-R (right) on the 400×400 2D Poisson benchmark distributed over 16 agents, with malevolent data corruption on agent 8 with $\omega_f = 2.5$ seconds, $\delta = 0.2$, and $\omega_r \in \{0.1, 0.2, 0.3, 0.4, 0.5\}$. The geometric mean of the relative error is reported for 10 runs per ensemble.

the malicious corruption was either too weak or too strong. The performance of ASJ-R might be further improved by developing either a better approximation to the shortest path length used in the rejection criterion or dynamic adjustments to the rejection criterion. A natural extension of this work is to apply similar modifications to more sophisticated iterative linear solvers such as the conjugate gradient method (CG). As a first step, we are developing a fully asynchronous variant of CG that relies on locally optimal direction vectors and extending our theoretical and empirical investigations on corruption resilience strategies in the context of the asynchronous CG algorithm.

REFERENCES

- [1] *Apache hadoop version 3.3.0.3*, 2021. <https://github.com/apache/hadoop>.
- [2] *Apache spark version 3.3.0*, 2021. <https://github.com/apache/spark>.
- [3] H. ANZT, J. DONGARRA, AND E. S. QUINTANA-ORTÍ, *Tuning stationary iterative solvers for fault resilience*, in Proceedings of the 6th Workshop on Latest Advances in Scalable Algorithms for Large-Scale Systems, Scala '15, New York, NY, USA, 2015, Association for Computing Machinery, <https://doi.org/10.1145/2832080.2832081>, <https://doi.org/10.1145/2832080.2832081>.
- [4] R. CANAL, C. HERNANDEZ, R. TORNERO, A. CILARDO, G. MASSARI, F. REGHENZANI, W. FORNACIARI, M. ZAPATER, D. ATIENZA, A. OLEKSIK, W. PIUNDEFINTEK, AND J. ABELLA, *Predictive reliability and fault management in exascale systems: State of the art and perspectives*, ACM Comput. Surv., 53 (2020), <https://doi.org/10.1145/3403956>, <https://doi.org/10.1145/3403956>.
- [5] D. CHAZAN AND W. MIRANKER, *Chaotic relaxation*, Linear Algebra and its Applications, 2 (1969), pp. 199–222, [https://doi.org/https://doi.org/10.1016/0024-3795\(69\)90028-7](https://doi.org/https://doi.org/10.1016/0024-3795(69)90028-7), <https://www.sciencedirect.com/science/article/pii/0024379569900287>.
- [6] Z. CHEN, *Online-abft: An online algorithm based fault tolerance scheme for soft error detection in iterative methods*, in Proceedings of the 18th ACM SIGPLAN Symposium on Principles and Practice of Parallel Programming, PPOPP '13, New York, NY, USA, 2013, Association for Computing Machinery, p. 167–176, <https://doi.org/10.1145/2442516.2442533>, <https://doi.org/10.1145/2442516.2442533>.
- [7] A. FROMMER AND D. B. SZYLD, *On asynchronous iterations*, Journal of Computational and Applied Mathematics, 123 (2000), pp. 201–216, [https://doi.org/https://doi.org/10.1016/S0377-0427\(00\)00409-X](https://doi.org/https://doi.org/10.1016/S0377-0427(00)00409-X), <https://www.sciencedirect.com/science/article/pii/S037704270000409X>.
- [8] J. HOOK AND N. DINGLE, *Performance analysis of asynchronous parallel jacobi*, Numerical Algorithms, 77 (2018), pp. 831–866, <https://doi.org/10.1007/s11075-017-0342-9>, <https://doi.org/10.1007/s11075-017-0342-9>.
- [9] *Ieee standard for floating-point arithmetic*, IEEE Std 754-2019 (Revision of IEEE 754-2008), (2019), pp. 1–84, <https://doi.org/10.1109/IEEESTD.2019.8766229>.
- [10] Q. LI, B. KAILKHURA, R. GOLDHAHN, P. RAY, AND P. K. VARSHNEY, *Robust decentralized learning using admm with unreliable agents*, 2018, <https://arxiv.org/abs/1710.05241>.

- [11] X. LIANG, J. CHEN, D. TAO, S. LI, P. WU, H. LI, K. OUYANG, Y. LIU, F. SONG, AND Z. CHEN, *Correcting soft errors online in fast fourier transform*, in Proceedings of the International Conference for High Performance Computing, Networking, Storage and Analysis, SC '17, New York, NY, USA, 2017, Association for Computing Machinery, <https://doi.org/10.1145/3126908.3126915>, <https://doi.org/10.1145/3126908.3126915>.
- [12] M. A. MUKWEVHO AND T. CELIK, *Toward a smart cloud: A review of fault-tolerance methods in cloud systems*, IEEE Transactions on Services Computing, 14 (2021), pp. 589–605, <https://doi.org/10.1109/TSC.2018.2816644>.
- [13] A. OLSHEVSKY, I. PASCHALIDIS, AND A. SPIRIDONOFF, *Fully asynchronous push-sum with growing intercommunication intervals*, 2018 Annual American Control Conference (ACC), (2018), pp. 591–596.
- [14] C. PONCE, *Skywing version 0.1.0*, July 2021. Github XXX.
- [15] J. WOLFSON-POU AND E. CHOW, *Convergence models and surprising results for the asynchronous jacobi method*, 2018 IEEE International Parallel and Distributed Processing Symposium (IPDPS), (2018), pp. 940–949.
- [16] P. WU, C. DING, L. CHEN, F. GAO, T. DAVIES, C. KARLSSON, AND Z. CHEN, *Fault tolerant matrix-matrix multiplication: Correcting soft errors on-line*, in Proceedings of the Second Workshop on Scalable Algorithms for Large-Scale Systems, Scala '11, New York, NY, USA, 2011, Association for Computing Machinery, p. 25–28, <https://doi.org/10.1145/2133173.2133185>, <https://doi.org/10.1145/2133173.2133185>.